

A Look at Some Data on the Old Faithful Geyser

By A. AZZALINI

University of Padua, Italy

and A. W. BOWMAN†

University of Glasgow, UK

[Received June 1988. Final revision August 1989]

SUMMARY

An analysis of data on the duration times and waiting times for eruptions from the Old Faithful Geyser reveals an interesting time series structure. A tentative physical model, derived from Rinehart, is outlined and a corresponding first-order Markov chain examined. It is shown that a second-order model is necessary to explain the observed correlations in the data. A curious clustering effect is apparent in the autocorrelation function when plotted over a large range of lags. Similar patterns are observed in simulations from the fitted second-order model.

Keywords: Autocorrelation; Markov chain; Time series

1. Introduction and Preliminary Analysis

This paper describes an analysis of some data on the Old Faithful Geyser in Yellowstone National Park, Wyoming, USA. The data consist of 299 pairs of measurements, referring to the time interval between the starts of successive eruptions w_i and the duration of the subsequent eruption d_i . Several similar data sets have been collected by the Park Geologist, R. A. Hutchinson. Weisberg (1980) and Denby and Pregibon (1987) analysed data collected in August 1978; Cook and Weisberg (1982) and Silverman (1985) referred to data collected in October 1980. Some background notes on the Old Faithful Geyser are provided by Rinehart (1969) and Birch and Kennedy (1972).

This analysis deals with data which were collected continuously from August 1st until August 15th, 1985. These data are listed in Table 1: because the unbroken sequence required measurements to be taken at night, some duration times are recorded as L (long), S (short) and M (medium). Other data sets do not contain a continuous stream of data, making it difficult to deal with time series features. A preliminary analysis of the 1980 data produced results that are very similar to some of those described in this paper.

†Address for correspondence: Department of Statistics, University Gardens, University of Glasgow, Glasgow, G12 8QW, UK.

TABLE 1
Duration d_i and waiting time w_i for the Old Faithful Geyser†

d_i	w_i	d_i	w_i	d_i	w_i	d_i	w_i	d_i	w_i	d_i	w_i
4:01	80	2:13	80	5:06	56	1:44	88	4:00	49	4:37	57
2:09	71	4:00	60	1:38	89	4:35	54	1:58	88	4:36	87
L	57	1:46	92	4:17	51	1:42	85	4:46	51	4:15	72
L	80	4:20	43	S	79	4:45	51	L	78	1:56	84
L	75	2:11	89	L	58	1:50	96	S	85	4:59	47
S	77	4:29	60	S	82	4:30	50	L	65	1:58	84
4:23	60	3:53	84	4:32	52	1:52	80	L	75	4:18	57
4:17	86	3:20	69	2:00	88	4:27	78	2:23	77	4:12	87
2:02	77	3:44	74	L	52	4:27	81	4:25	69	4:32	68
4:50	56	4:00	71	2:56	78	4:00	72	4:13	92	4:24	86
1:50	81	1:57	108	4:44	69	4:48	75	4:22	68	4:37	75
5:27	50	5:16	50	3:54	75	L	78	2:00	87	S	73
1:37	89	S	77	1:57	77	L	87	4:27	61	L	53
4:52	54	L	57	4:07	53	S	69	1:45	81	L	82
4:23	90	S	80	1:48	80	L	55	4:30	55	3:55	93
1:46	73	L	61	4:40	55	1:56	83	1:37	93	S	77
4:40	60	S	82	1:50	87	4:35	49	4:42	53	4:30	54
S	83	L	48	4:42	53	2:00	82	2:34	84	1:48	96
4:44	65	3:32	81	2:07	85	3:42	57	3:42	70	4:00	48
4:13	82	2:10	73	4:47	61	2:52	84	4:14	73	2:45	89
1:54	84	4:30	62	1:49	93	4:50	57	1:56	93	4:44	63
4:58	54	2:01	79	4:06	54	3:27	84	4:21	50	3:58	84
S	85	4:09	54	4:39	76	4:23	73	L	87	1:57	76
L	58	4:12	80	L	80	1:48	78	L	77	4:58	62
S	79	4:20	73	S	81	4:24	57	L	74	1:51	83
L	57	1:56	81	L	59	2:29	79	4:13	72	4:48	50
2:50	88	4:39	62	L	86	4:31	57	4:00	82	L	85
4:30	68	3:49	81	4:13	78	2:06	90	4:08	74	L	78
4:04	76	4:02	71	4:08	71	4:21	62	1:53	80	L	78
3:43	78	4:10	79	3:56	77	4:22	87	4:28	49	L	81
3:31	74	4:40	81	3:45	76	1:47	78	1:57	91	L	78
4:28	85	1:49	74	4:25	94	4:55	52	4:13	53	L	76
2:13	75	L	59	2:28	75	1:49	98	1:43	86	L	74
4:53	65	M	81	4:10	50	L	48	4:27	49	S	81
2:36	76	L	66	3:48	83	L	78	4:15	79	L	66
4:09	58	S	87	4:19	82	L	79	3:58	89	1:56	84
2:12	91	4:27	53	3:52	72	3:52	65	4:23	87	4:20	48
4:46	50	2:03	80	4:41	77	1:51	84	1:58	76	1:40	93
1:50	87	4:15	50	1:42	75	4:42	50	4:27	59	4:46	47
4:36	48	1:55	87	4:58	65	2:01	83	4:16	80	1:57	87
2:16	93	4:40	51	4:16	79	4:28	60	1:55	89	4:41	51
4:08	54	1:44	82	4:35	72	1:52	80	4:25	45	1:56	78
S	86	4:23	58	L	78	4:10	50	M	93	4:25	54
L	53	1:46	81	L	77	1:54	88	L	72	2:08	87
S	78	4:36	49	L	79	4:15	50	S	71	4:05	52
L	52	1:52	92	L	75	3:15	84	L	54	2:04	85
1:53	83	4:27	50	1:59	78	4:13	74	3:17	79	L	58
4:16	60	1:38	88	4:36	64	1:53	76	1:50	74	L	88
2:05	87	5:02	62	0:50	80	4:59	65	4:37	65	S	79
4:28	49	1:49	93	4:55	49	1:51	89	1:50	78		

† Read columnwise. Units are minutes:seconds, minutes. S means short, L means long and M means medium.

In previous publications, regression models are fitted to data in the form of Fig. 1 to predict w_{t+1} from d_t : groups A, B and C are described later. Some researchers show how a cursory analysis of regression residuals may fail to detect the presence of two separate clusters. For plotting and subsequent analysis, the codes L, S and M are represented numerically as 4, 2 and 3 respectively.

We start by observing that the data consist of two interwoven time series, $\{d_t\}$ and $\{w_t\}$. Fig. 2 displays the first 100 observations of $\{d_t\}$ plotted against event number; the remaining 199 values, and the plot of $\{w_t\}$, behave similarly. These series exhibit highly oscillatory behaviour, essentially alternating between two levels. A closer look shows that a low level is always followed by a high level, and a high level is very often, but not always, followed by a low level.

A simple consideration of the physical mechanism suggests that the relationship between d_t and w_t is important: w_t is the length of time taken to heat the water to be expelled over the interval d_t . Since the $\{w_t\}$ values are the interval times between the starts of the eruptions, w_t exceeds the actual waiting time. However, the difference is unimportant as d_t is considerably smaller than w_t in magnitude. Fig. 3 plots d_t versus w_t and shows clearly the existence of three separate clusters, A, B and C, corresponding approximately with divisions at 3 and 68 on the d_t and w_t axes. There is now less evidence of a relationship between d_t and w_t within each cluster. Also, a short waiting time is always followed by a long eruption time but a long waiting time is followed by short and long eruption times in roughly equal proportions. Consequently, to understand the mechanism of the series we consider the joint behaviour of at least the three variables (w_t, d_t, w_{t+1}). Figs 1 and 3 display two of the possible bivariate plots. The pattern of the third, w_{t+1} against w_t , is virtually the same as Fig. 3. Happily, the special nature of the groupings within these projections allows the three-dimensional pattern to be identified, as in Fig. 4, where only three clouds (A, B, C) are evident.

Fig. 1 is the projection of these clouds on to the (w_{t+1}, d_t) plane. The regression effect at the upper level is enhanced by the superposition of clouds A and B which have a slight relative shift. The regression effect of waiting time on previous duration time

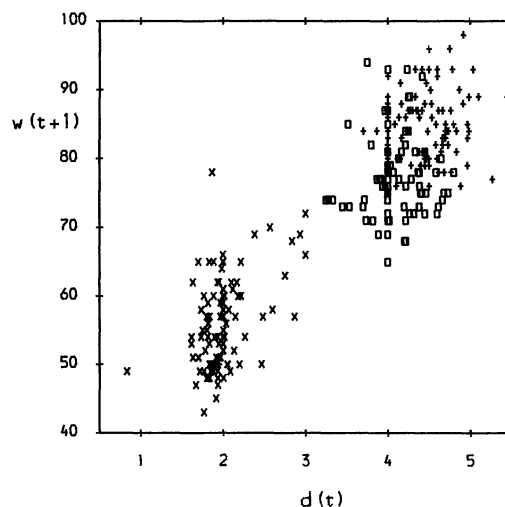


Fig. 1. Waiting time w_{t+1} versus previous duration d_t : +, group A; □, group B; ×, group C

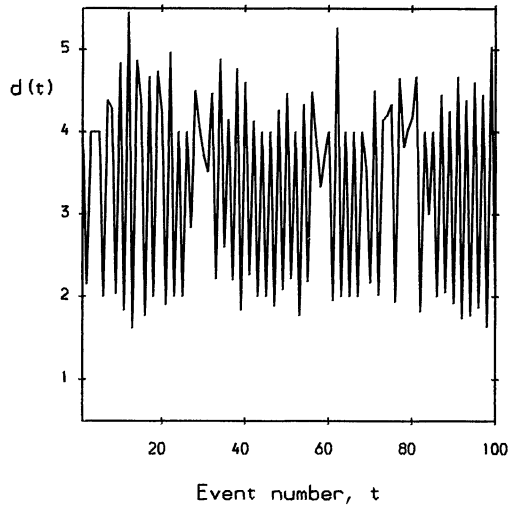


Fig. 2. Duration d_t versus event number t

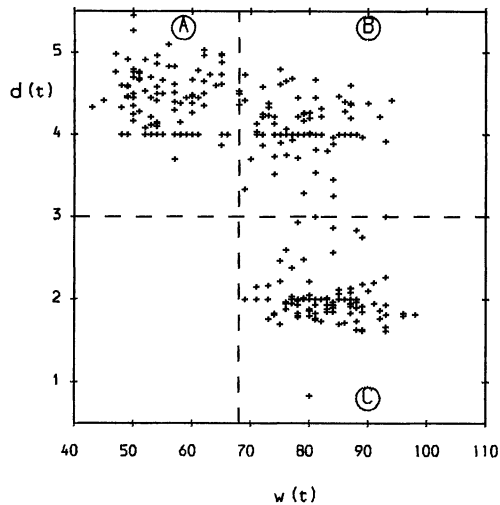


Fig. 3. Duration d_t versus previous waiting time w_t

is greatly reduced for each group. A small effect persists but a formal assessment of its significance is hindered by autocorrelation among the data.

2. Tentative Physical Model

The existence of two distinct patterns in a geyser's behaviour is rare. The following description of a conceivable scheme is based on Rinehart (1969), pp. 571–573, and is illustrated by Fig. 5 (Rinehart (1969), p. 572).

Stage 1. The tube is full of water which is heated by the surrounding rocks. The water is heated above the normal boiling temperature because of increased pressure

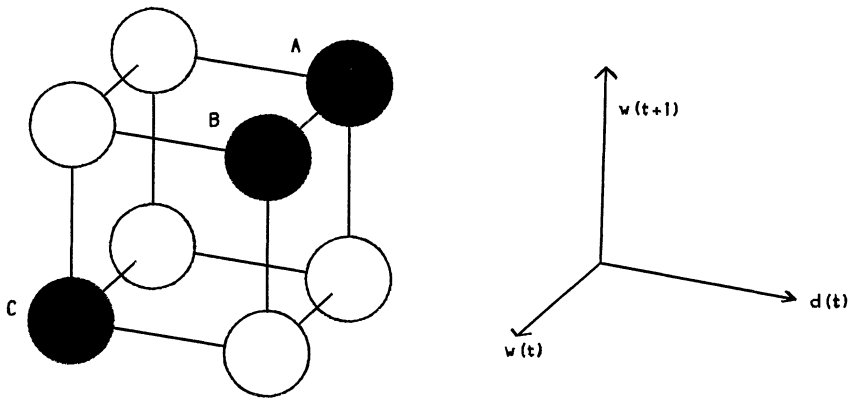


Fig. 4. Sketch of the three-dimensional configuration among $\{w_t, d_t, w_{t+1}\}$

due to the mass of water which is on top: the deeper the water the higher the temperature required for boiling. Moreover, 'whereas the water in the tube is superheated with respect to the ambient boiling point at the mouth of the geyser, the water temperature at depth is far below the boiling point curve that must be applied to a vertical column of water'.

Stage 2. When the top water reaches the boiling temperature, it becomes steam and moves towards the surface. The pressure at the bottom then drops rapidly to the normal level and, by an induction effect, the bottom water rapidly becomes steam. This cascading mechanism is repeated several times: as water is converted into steam, the pressure on lower water is decreased, causing the production of more steam and triggering the eruption.

Stage 3a. 'If at the time of cascading the temperature in the lower regions is lower than might be expected, cascading stops short of the bottom and the play is short.'

Stage 3b. Alternatively, 'when the temperature is comparatively high at these depths, cascading works itself down much farther and the play is long'.

Stage 4. The geyser tube is completely or partly empty, ready to be filled with new water.

We do not discuss geological reasons for the fact that sometimes the cascading effect works down to the bottom of the tube while at other times it stops earlier. We simply note the phenomenon and discuss its consequences. Stages 3a and 3b are associated with short and long waiting times for the next eruption. In stage 3a, the system starts a new cycle partially filled with hot water so that the following heating time is shorter; at the new eruption the entire tube will be emptied, since part of the water had already been heated in the previous cycle.

This description suggests a two-state Markov chain as a model for the oscillations between the high and low levels and implies that the variables d_t and w_{t+1} may be regarded as equivalent indicators of the state of the system. This is corroborated by Fig. 1, where low d_t is associated with low w_{t+1} , and high d_t with high w_{t+1} : see also Fig. 9 of Denby and Pregibon (1987), where plots of $\{d_t\}$ and $\{w_{t+1}\}$ against event number are superimposed. Finally, the cross-correlation between the two series is found to be highly symmetrical about zero, implying that the series are 'in phase'.

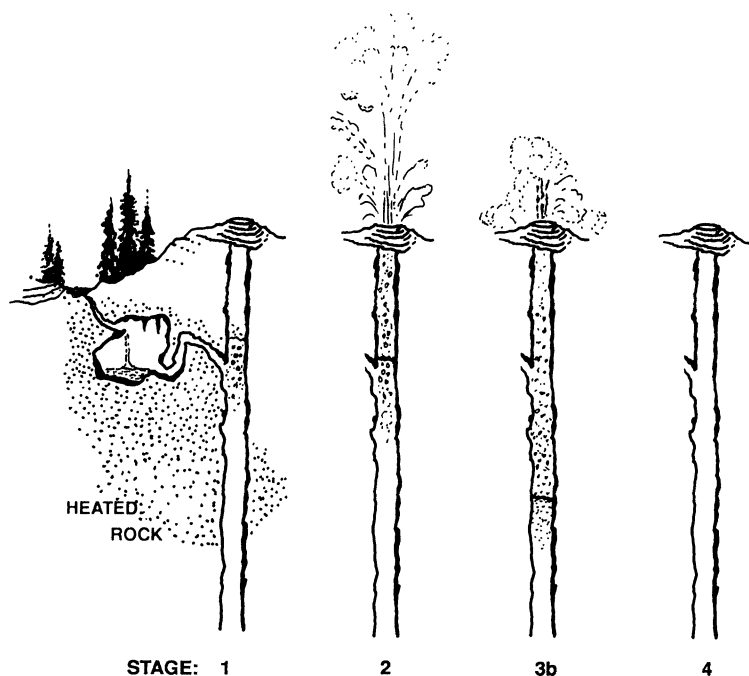


Fig. 5. Sketch of the conjectured geyser mechanism (from Rinehart (1969))

The original data are discretized to low-high form by division at 3 and 68 on the original scales, associating the numerical values 0 and 1 to low and high respectively for convenience. Denoting by $\{D_t\}$ and $\{W_t\}$ the two discretized processes, the (i, j) th entry of the Markov transition matrix P_D of $\{D_t\}$ gives

$$\text{pr}\{D_t = j | D_{t-1} = i\} \quad (i = 0, 1; \quad j = 0, 1)$$

and similarly for $\{W_t\}$. Standard estimation of the transition matrices leads to

$$P_D = \begin{pmatrix} 0 & 1 \\ 0.557 & 0.443 \end{pmatrix}, \quad P_W = \begin{pmatrix} 0 & 1 \\ 0.536 & 0.464 \end{pmatrix}$$

while the relative frequencies of high states are

$$p_D = 0.641, \quad p_W = 0.651$$

for $\{D_t\}$ and $\{W_t\}$ respectively. These matrices and frequencies are clearly similar.

Such a discretization of the data ignores some information. However, the alternation between the two levels is the most important feature and the variation within groups is comparatively small, as the summary statistics in Table 2 show.

In view of these remarks and the equivalence between $\{d_t\}$ and $\{w_t\}$, we concentrate on the discretized process $\{D_t\}$.

3. Second-order Model

A check on the adequacy of the model can be obtained by comparing the observed autocorrelations with those obtained under the Markov assumption. The first eight

TABLE 2

Summary statistics for $\{d_t\}$ and $\{w_t\}$

	Mean	$\{d_t\}$ Standard deviation	Mean	$\{w_t\}$ Standard deviation
Pooled groups	3.460	1.154	72.174	13.916
Low group	1.977	0.275	55.020	5.618
High group	4.262	0.413	81.056	6.763

terms of the observed autocorrelation function (ACF) and partial autocorrelation function (PACF) for the $\{D_t\}$ process are as follows:

lag	1	2	3	4	5	6	7	8
ACF	-0.538	0.478	-0.346	0.318	-0.256	0.208	-0.161	0.136
PACF	-0.538	0.266	-0.021	0.075	-0.021	-0.009	0.010	0.006

The ACF clearly does not show the geometric decay which would be expected under a Markov model. Moreover, while the PACF after lag 1 should be close to zero, the second term of the PACF is high when compared with the usual standard error for an autoregressive series (0.058).

The ACF and PACF given above point towards a second-order Markov chain. An estimate of the corresponding transition matrix for $\{D_t\}$ is

$$\begin{array}{cc}
 & \begin{matrix} (0, 1) & (1, 0) & (1, 1) \end{matrix} \\
 \begin{matrix} (0, 1) \\ (1, 0) \\ (1, 1) \end{matrix} & \begin{pmatrix} 0 & 0.689 & 0.311 \\ 1 & 0 & 0 \\ 0 & 0.388 & 0.612 \end{pmatrix}
 \end{array} \quad (1)$$

where the three states correspond to (low, high), (high, low) and (high, high), and the (low, low) state cannot occur. This confirms that the first-order model is inadequate. If a third-order Markov chain is fitted, the estimates produced are consistent with a second-order model.

Under the assumption of a second-order Markov chain with transition matrix (1), a standard computation of the stationary probabilities for the (0, 1), (1, 0) and (1, 1) states gives 0.357, 0.357 and 0.286, so that the stationary probability of the high state is $0.357 + 0.286 = 0.643$ as before, but now there is a much closer agreement with the autocorrelation pattern: computation of the first eight terms of the theoretical ACF under model (1) gives

$$-0.558 \quad 0.515 \quad -0.368 \quad 0.300 \quad -0.227 \quad 0.179 \quad -0.137 \quad 0.108$$

which are in close agreement with the observed terms.

However, the first few terms of the ACF and PACF reveal only part of the picture. A plot of the ACF of the original discretized data over a much wider range is given in Fig. 6, from which it is clear that the correlations do not go to zero at high lags. There is a clear recurrent clustering effect. A very similar picture is obtained from the $\{W_t\}$ process.

To check the fitted model, several series of length 299 were simulated from the fitted second-order Markov chain. The random number generator of Wichmann and

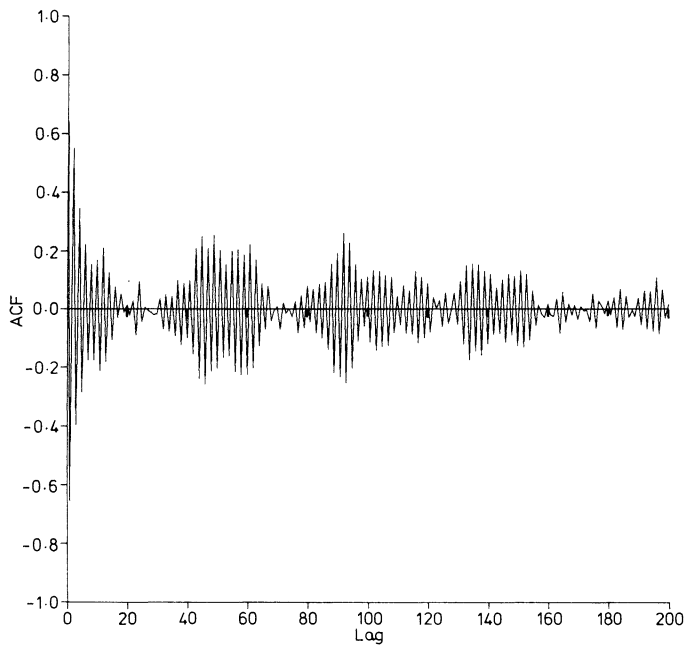


Fig. 6. Autocorrelation function of $\{D_t\}$

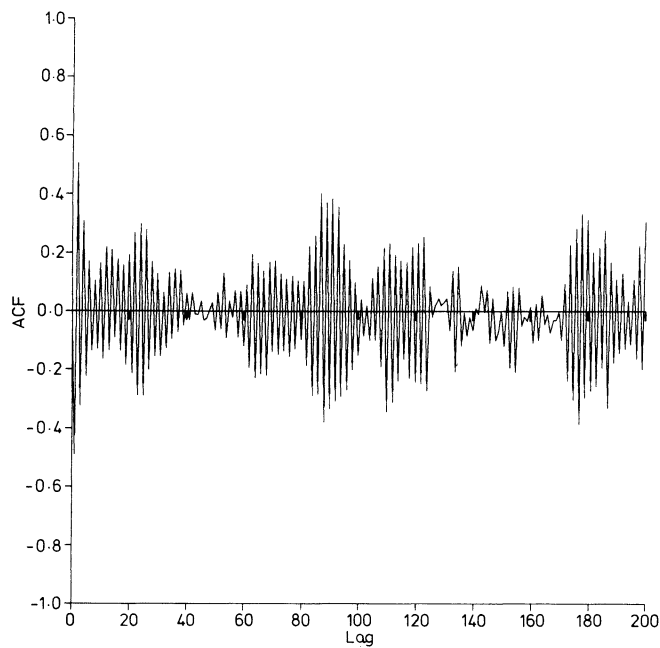


Fig. 7. Autocorrelation function of data simulated from the fitted second-order Markov chain

Hill (1982) was used. The ACF of one of these series (Fig. 7) is qualitatively similar to that of the observed $\{D_t\}$ process. The simulations showed great variability in the number, locations and widths of the clusters. It was necessary to increase the length of the simulated series to 5000 before the clusters disappeared, leaving only the first 20 terms decreasing regularly to zero. The presence of these clusters in the observed ACF therefore does not provide convincing evidence of a failure of the model, as it is consistent with fluctuations which arise from sampling errors.

The tentative physical model explains several features of the data but does not explain the patterns of the ACF and PACF. These are consistent with a second-order Markov chain, which requires a more sophisticated geological interpretation. Although the oscillations of the ACF are consistent with a second-order Markov chain model, only the analysis of a much longer series of data may rule out the existence of more complex patterns.

Acknowledgements

We are very grateful for the extensive help of R. A. Hutchinson and to G. Bellieni for additional advice on geological aspects. The helpful comments of S. Weisberg, B. W. Silverman, G. Masarotto, D. Vere-Jones and two referees were much appreciated. The support of the Science and Engineering Research Council, the British Council and the Italian Ministry of Education in financing visits between Padua and Glasgow is gratefully acknowledged.

References

- Birch, F. and Kennedy, G. C. (1972) Notes on geyser temperature in Iceland and Yellowstone National Park. In *Geophysical Monograph Series*, vol. 16, *Flow and Fracture Rocks* (eds H. C. Heard, I. Y. Borg, N. L. Carter and C. B. Raleigh), pp. 329–336. Washington DC: American Geophysical Union.
- Cook, R. D. and Weisberg, S. (1982) *Residuals and Influence in Regression*. London: Chapman and Hall.
- Denby, L. and Pregibon, D. (1987) An example of the use of graphics in regression. *Am. Statistn*, **41**, 33–38.
- Rinehart, J. S. (1969) Thermal and seismic indications of Old Faithful Geyser's inner working. *J. Geophys. Res.*, **74**, 566–573.
- Silverman, B. W. (1985) Some aspects of the spline smoothing approach to non-parametric regression curve fitting (with discussion). *J. R. Statist. Soc. B*, **47**, 1–52.
- Weisberg, S. (1980) *Applied Linear Regression*, pp. 207–211. New York: Wiley.
- Wichmann, B. A. and Hill, I. D. (1982) Algorithm AS 183: An efficient and portable pseudo-random number generator. *Appl. Statist.*, **31**, 188–190.